JOURNAL OF APPLIED ELECTROCHEMISTRY 20 (1990) 347–356

REVIEWS OF APPLIED ELECTROCHEMISTRY 22

The electrochemical facetting of metal surfaces: Preferred crystallographic orientation and roughening effects in electrocatalysis

W. E. TRIACA, A. J. ARVIA

Instituto de Investigaciones Fisicoquímicas Teóricas y Aplicadas – INIFTA, Facultad de Ciencias Exactas, Universidad Nacional de La Plata, Sucursal 4, Casilla de Correo 16, (1900) La Plata, Argentina

Received 15 September 1988; revised 22 June 1989

New electrochemical procedures to develop highly rough and preferentially oriented surfaces at face-centered cubic metals are described. The structure and morphology of the different surfaces have been studied through scanning electron and scanning tunneling microscopy. The mechanisms of the processes involved in the development of roughening and preferred crystallographic orientation are discussed on the basis of electrochemical data for platinum in acid electrolytes. The electrochemical behaviour of the new electrode surfaces has been tested for different reactions, such as the electrooxidation of adsorbed carbon monoxide on preferentially oriented platinum and the adsorption and electrooxidation of both ethylene and reduced carbon dioxide on electrodispersed platinum.

1. Introduction

The development of solid metal catalysts with optimal performance for heterogeneous reactions firstly requires the knowledge of the concentration and the energy distribution of the proper active sites. In addition the metal catalysts should provide large active areas involving an adequate structure to achieve the fastest entrance and most uniform accessibility of reactants, and the greatest and most rapid removal of products. Despite the outstanding contributions made in recent years the present state of knowledge on the matter is limited in comparison to the wide use of metals and their compounds in heterogeneous catalysis including electrocatalysis.

The behaviour of polycrstalline (pc) metal surfaces in adsorption/desorption electrochemical processes reveals that they are susceptible to remarkable changes in surface roughness and in the distribution of crystallographic faces after the application of periodic perturbing potentials [1–10]. These changes, namely, roughening and facetting with preferred crystallographic orientation (pco), can be voltammetrically followed in the potential range of H- and O-electrosorption for different fcc metals. Both the rough and facetted metal surfaces are very reproducible and promising for investigating reactions of different adsorbates at well defined metal substrates. The present work refers to the development of these new techniques and to the application of modified metal surfaces to various reactions of interest in electrocatalysis.

2. Electrochemical procedures to change roughness and crystallographic orientation of fcc metal surfaces

The surface of a fcc metal electrode immersed in aqueous solutions can be substantially modified in different ways through the application of periodic perturbing potentials (Fig. 1), namely, by increasing the real surface area [1, 2, 4, 10], by changing the relative proportion of crystallographic faces [3–12] and by producing a particular surface morphology [12]. The prevailing type of change depends principally on the potential limits and frequency of the periodic potential, and secondarily on the waveform and the electrolyte composition [4, 9]. It is also possible to accomplish a combined effect such as the development of a particular preferred crystallographic orientation, and simultaneously a substantial increase in real surface area [12, 13]. These results offer, for the first time, the possibility of a rational handling of the two most important characteristics of the surface of metal electrodes, namely, type and density of reacting sites, through an electrode treatment under definite operating conditions.

In general, the electrochemical procedures to change either the roughness or the distribution of crystallographic faces at the metal surface, or both at the same time, can be distinguished as follows:

(i) metal electrodeposition under modulated potential conditions [6];

(ii) cyclic fast electroformation and partial electroreduction of thick oxide layers followed by slow electroreduction scans [1, 2, 10];

(iii) cyclic fast electroadsorption and electrodesorption of H-atoms and oxygen-containing species at room temperature [3–5, 9, 14–16];

(iv) cyclic potential perturbation at relatively high temperature by using a molten electrolyte [17];

(v) combinations of low and high frequency periodic perturbing potentials [13].

The efficiency of each procedure is strongly depen-

0021-891X/90 $03.00 + .12

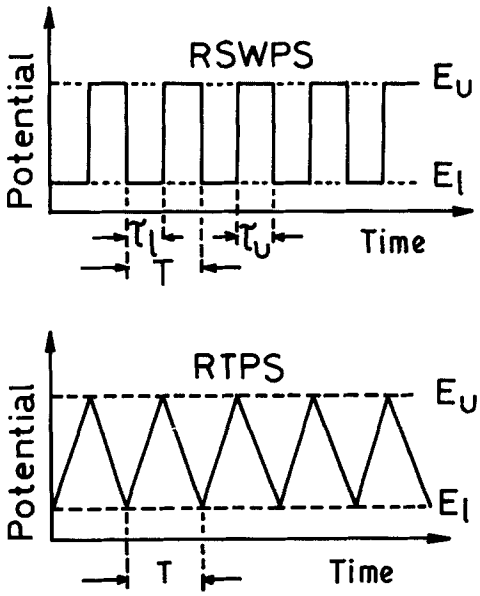

Fig. 1. Scheme of typical periodic perturbing potentials. RSWPS = repetitive square wave potential signal; RTPS = repetitive triangular potential signal; T = period; τ_l = cathodic half-period; τ_u = anodic half-period; E_l = lower potential limit; E_u = upper potential limit.

dent on both the frequency and the potential window of the perturbing potential involved. Thus, remarkable increases in real surface area of pc platinum, pc rhodium and pc gold electrodes can be accomplished through the electroreduction of relatively thick oxide layers (in the order of 1 μm) produced by a repetitive square wave potential signal (RSWPS) of suitable upper (E_u) and lower (E_l) potential limits and frequency (f) (Procedure ii). The useful ranges of RSWPS parameters are as follows:

(a) for platinum: $2.0\,V \leqslant E_u \leqslant 2.8\,V$; $-0.3\,V \leqslant E_l \leqslant 0.5\,V$; $0.5\,kHz \leqslant f \leqslant 10\,kHz$;

(b) for rhodium: $1.9\,V \leqslant E_u \leqslant 2.3\,V$; $-0.1\,V \leqslant E_l \leqslant 0.1\,V$; $0.5\,kHz \leqslant f \leqslant 6\,kHz$;

(c) for gold: $2.1\,V \leqslant E_u \leqslant 3.0\,V$; $0.2\,V \leqslant E_l \leqslant 1.1\,V$; $1.0\,kHz \leqslant f \leqslant 10\,kHz$.

The increase in active area (R) of the treated surface can be voltammetrically determined by comparing, before and after the application of the perturbing potential, either the corresponding H-adatom monolayer electroformation charge or the electroreduction charge of the O-adatom monolayer. An illustrative example of increase in active surface area for platinum is given in Fig. 2.

On the other hand, facetted metal surfaces with pco involving no appreciable change in roughness can be obtained through the application of fast perturbing potentials to either pc or polyfacetted single crystal (sc) metal electrodes (Procedure iii). The change in the distribution of the different crystallographic faces produces a modification in the relative height of voltammetric current peaks related to the H-adatom reaction as for instance platinum and rhodium in acid solutions [3–5, 9, 15, 16] (Figs. 3 and 4). The degree of development of (100)-type pco of the treated surface can be voltammetrically followed as the ratio between the height of the strongly adsorbed H-electrooxidation

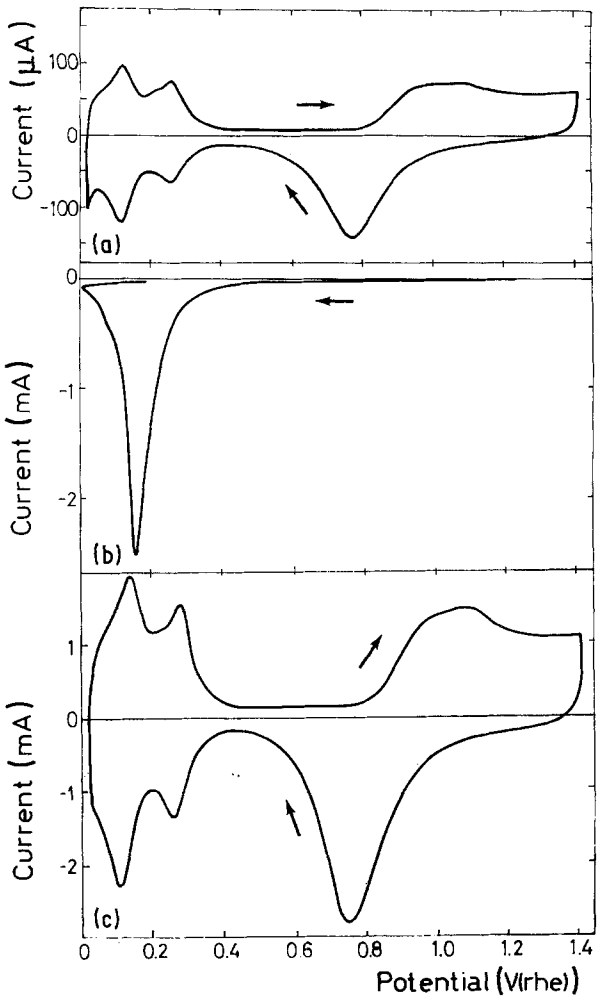

Fig. 2. Voltammograms of platinum electrodes in 0.5 M H_2SO_4 at 30° C. (a) Starting electrode after 5 min cycling at $0.3\,V\,s^{-1}$; (b) electroreduction profile made at $3 \times 10^{-3}\,V\,s^{-1}$ immediately after the RSWPS treatment (E_u = 2.4 V; E_l = 0.4 V; f = 1.8 kHz; time = 3 min); (c) electrodispersed platinum electrode after 5 min potential cycling at $0.3\,V\,s^{-1}$. r.h.e. = reversible hydrogen electrode (reference potential).

current peak (h_2) and the height of the weakly adsorbed H-electrooxidation current peak (h_1). Likewise, the degree of voltammetric change associated with the (111)-type pco is arbitrarily given in terms of the ratio h_1/h_2. As an example, the optimal RSWPS parameters for 100-type facetting of platinum are: E_u = 1.50 V, E_l = 0.05 V and f = 7 kHz. In this case (Fig. 3), the voltammogram at $0.1\,V\,s^{-1}$ for H-atom electrosorption in acid approaches those reported in the literature for either platinum (100) sc surfaces or platinum sc stepped surfaces with (100) narrow terraces under comparable conditions [18–21]. Likewise, the optimal conditions for (111)-type facetting are: E_l = 0.70 V, E_u = 1.35 V and f = 7 kHz. The voltammetric response at $0.1\,V\,s^{-1}$ between 0.05 and 0.60 V of the treated electrode surface in acid (Fig. 4) approaches those reported for either platinum (111) sc surfaces or platinum sc stepped surfaces with (111) narrow terraces under comparable conditions [20–28]. Comparable electrochemical facetting conditions have also been established for rhodium, gold and palladium and to some extent for silver, nickel and copper.

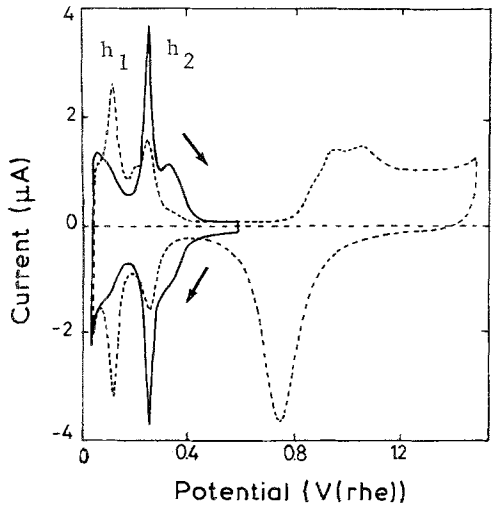

Fig. 3. Voltammograms at 0.1 V s^{-1} of platinum electrodes in 0.5 M H_2SO_4 at 25° C. Dashed trace corresponds to a polished pc platinum electrode. Full trace belongs to a (100)-type preferentially oriented platinum electrode resulting from Procedure (iii). Peak h_1 corresponds to weakly bonded H-adatoms and peak h_2 to strongly bonded H-adatoms.

Another procedure was also developed to produce the two effects on the same substrate in such a way that the active surface area increase and the electrochemical facetting with pco take place along with the global treatment under controlled conditions (Procedure v) [13]. In this technique, the metal electrode is subjected to a relatively low frequency (f_1) RSWPS between preset E_u and E_l for a time t_1 and immediately afterwards a second RSWPS at a higher frequency (f_2) is applied for a time t_2 between the same potential limits (Fig. 5a). The low frequency RSWPS mainly produces the increase in active surface area (Fig. 5b), whereas the fast RSWPS is responsible for the development of the pco (Fig. 5c). A good example of this procedure is the remarkable increase in active surface area of platinum and the development of (100)-type facetting which can be obtained under the following conditions: E_u = 1.4 V, E_l = 0.0 V, f_1 = 0.025 kHz, t_1 = 5 h, f_2 = 4 kHz and t_2 = 5 h. Likewise, the increase in active surface area together with the development of (111)-type facetting can be accomplished through a combined RSWPS treatment with the following characteristics: E_u = 1.35 V, E_l = 0.70 V, f_1 = 1.2 kHz, t_1 = 4.5 h, f_2 = 6 kHz and t_2 = 4 h.

Other combinations of periodic perturbing potentials including changes in the symmetry of the RSWPS, also are useful for the achievement of large active surface areas with particular pco [12].

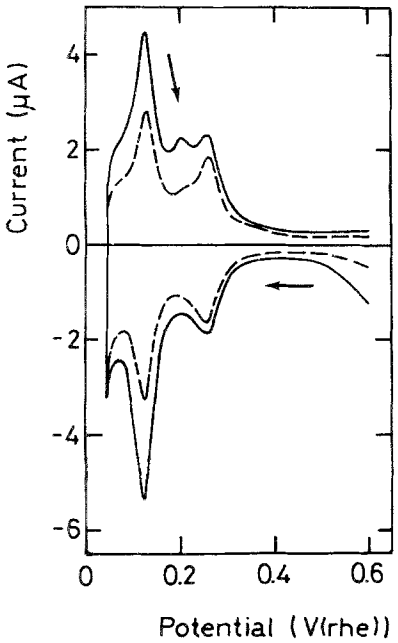

Fig. 4. Voltammograms at 0.1 V s^{-1} of platinum electrodes in 1 M H_2SO_4 at 25° C. Dashed trace corresponds to an untreated polyfacetted sc platinum electrode. Full trace belongs to a (111)-type preferentially oriented platinum electrode resulting from Procedure (iii).

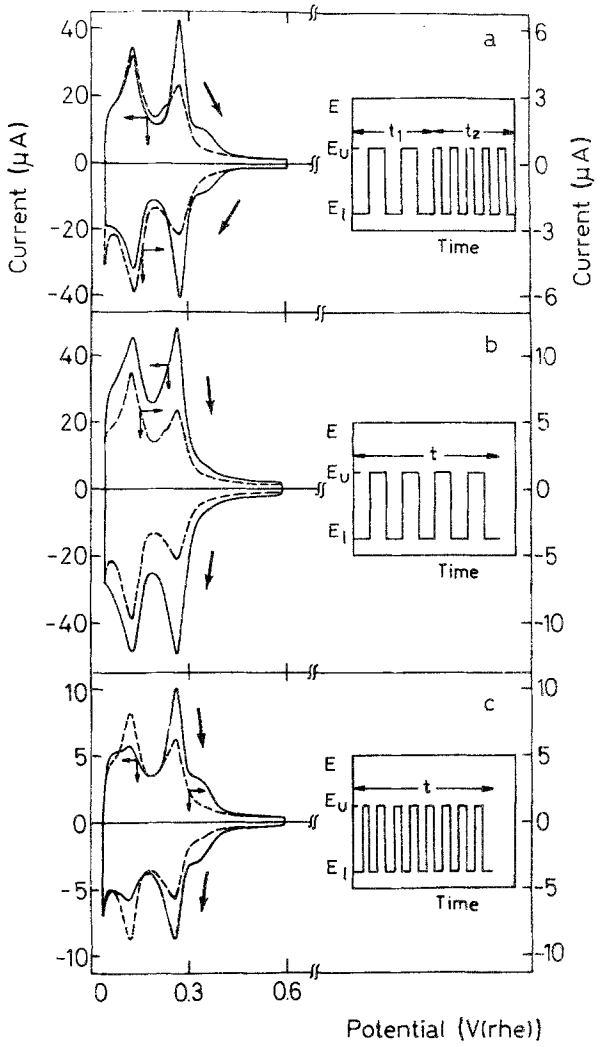

Fig. 5. Voltammograms at 0.3 V s^{-1} in 1 M H_2SO_4 at 25° C. Dashed traces correspond to untreated platinum electrodes. Full traces: (a) after a combined RSWPS treatment (E_l = 0 V; E_u = 1.4 V; f_1 = 25 Hz; t_1 = 5 h; f_2 = 4 kHz; t_2 = 5 h); (b) after a single RSWPS treatment (E_l = 0 V; E_u = 1.4 V; f = 25 Hz, t = 5 h); (c) after a single RSWPS treatment (E_l = 0 V; E_u = 1.4 V; f = 4 kHz; t = 5 h). The potential/time programs applied to the electrodes are also depicted for each figure.

3. SEM and STM imaging of electrochemically modified metal surfaces

Scanning electron microscopy (SEM) and scanning tunneling microscopy (STM) images display typical

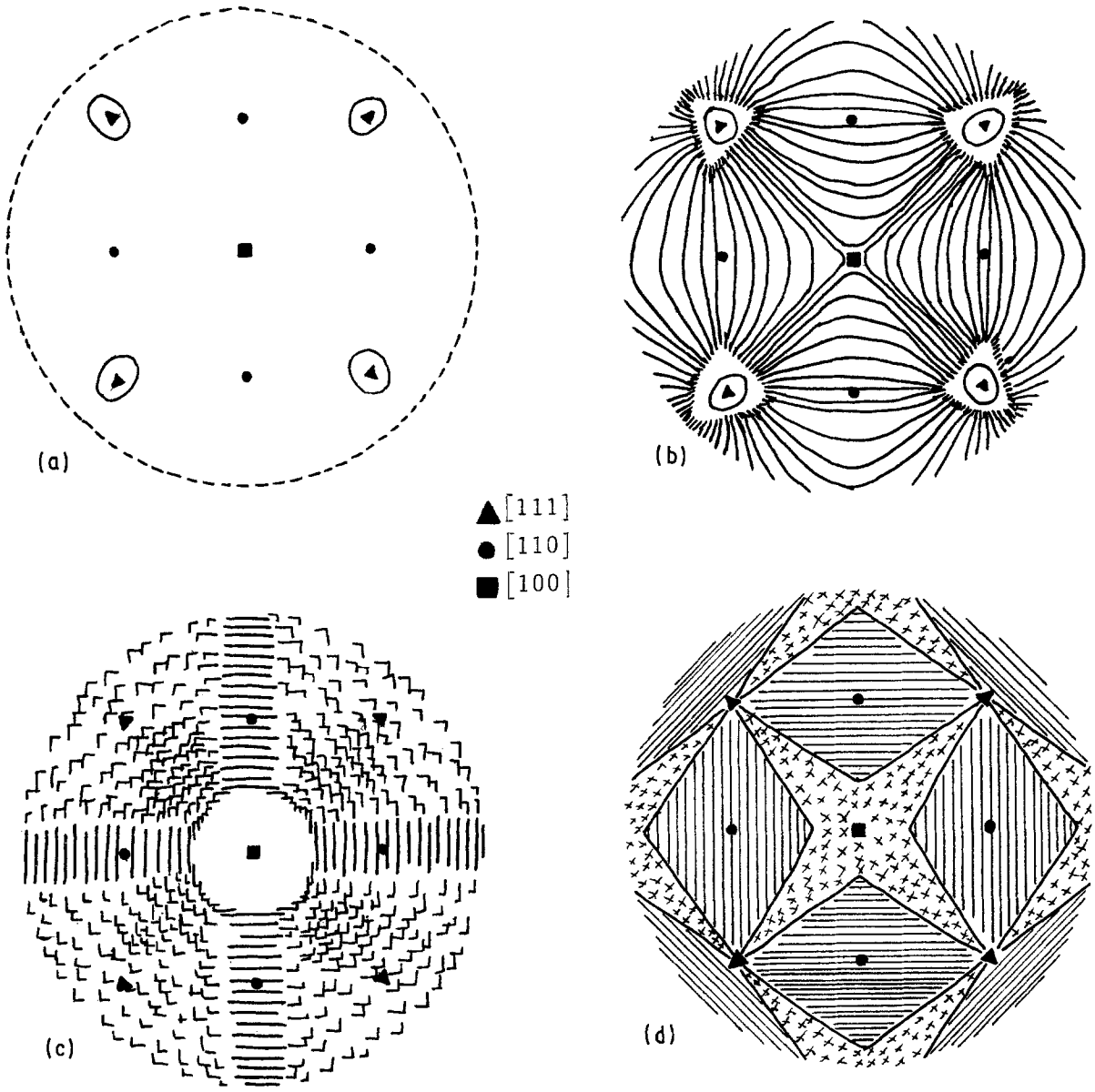

Fig. 6. Scheme of observed SEM patterns for a sc fcc metal sphere after electrochemical facetting: (a) untreated polyfacetted sc sphere; (b) (111)-type pco; (c) (100)-type pco; (d) (110)-type pco. (Reproduced by kind permission of Elsevier Sequoia SA).

surface topographies at the micron and nanometer ranges, respectively.

After electrochemical facetting under properly chosen conditions a small spherical sc platinum surface initially polyfaceted shows SEM micrographs corresponding to the development of either (111), (100) or (110) pco [14] (Fig. 6). Comparable results are obtained by starting from a pc platinum surface [9, 29]. In this case, the development of large grains and net grain boundaries can be observed (Fig. 7), each grain exhibiting the typical facetting of a particular preferred orientation [9].

The STM images of the electrochemically facetted specimens [30], for instance, that of a platinum surface involving (100)-type pco show a very smooth surface with a prevalence of parallel ridges ranging from 5 to 10 nm height (Fig. 8). Other regions show a clear development of smooth square terraces. The entire topography is similar to that reported for platinum (100) sc in air [31].

Otherwise, for highly rough electrode surfaces one obtains SEM micrographs with a cauliflower structure [32] (Fig. 9). Correspondingly, the STM images of these surfaces [33, 34] reveal three features (Fig. 10), namely, large steps and irregularities, flat regions with parallel steps similar to those described for electrochemically facetted pco specimens, and regions with casket-like structures which constitute the major contribution for the increase in surface roughness. The model for describing the behaviour of these electrodes, as derived from both STM and electrochemical data, consists of sticking pebble-like platinum superclusters of about 10 nm diameter (Fig. 11), which originate an inner channel-like structure, enabling practically the entire surface of each pebble to become accessible for reactants, at least for small size molecules. A full account of these results is given elsewhere [33, 34].

4. The mechanism of electrochemical facetting

The mechanism of the electrochemical facetting yielding pco is strongly dependent on the potential window

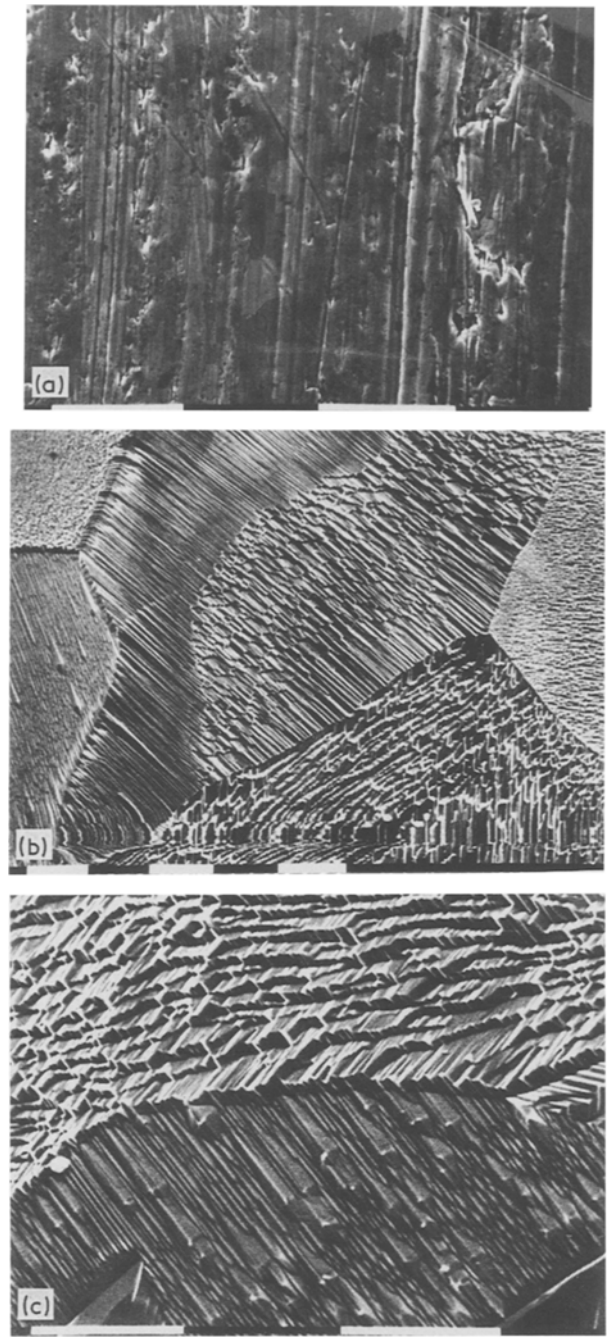

Fig. 7. SEM micrographs (scale 10 μm): (a) initial electropolished pc platinum; (b), (c) platinum surface after 4 h RSWPS (E_l = 0.25 V; E_u = 1.25 V; f = 4 kHz) in 1 M H_2SO_4 at 25° C. RSWPS conditions were chosen to develop the (100)-type pco.

and frequency of the periodic perturbing potential as both parameters determine the prevailing faradaic processes proceeding at the upper (E_u) and the lower (E_l) potential limits, respectively. As a first approach a prediction of the likely electrochemical processes can be cautiously derived from thermodynamics taking

Table 1. Standard electrode potentials related to platinum [35, 36]

$Pt^{2+} + 2e^- = Pt$	E_1° = 1.188 V
$Pt(OH) + H^+ + e^- = Pt + H_2O$	E_2° = 0.850 V
$PtO + 2H^+ + 2e^- = Pt + H_2O$	E_3° = 0.980 V
$PtO_2 + 2H^+ + 2e^- = PtO + H_2O$	E_4° = 1.045 V
$PtO_2 + 4H^+ + 2e^- = Pt^{2+} + 2H_2O$	E_5° = 0.837 V

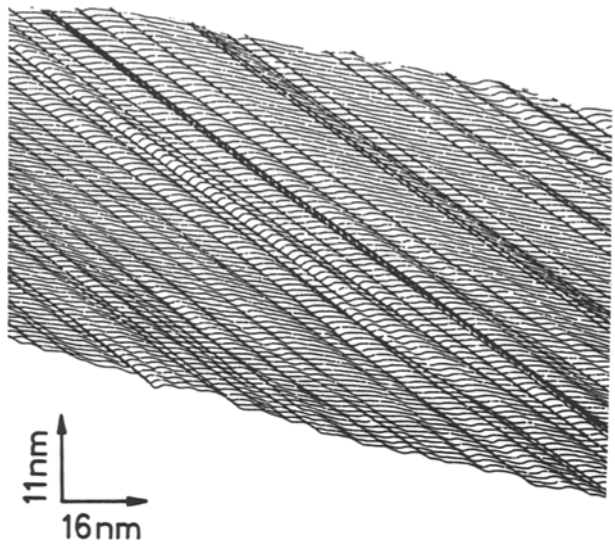

Fig. 8. STM image of a platinum surface resulting after electrochemical treatment yielding the (100)-type pco.

into account the redox couples involving oxidized and reduced metal species [35, 36]. Thermodynamic data related to platinum as example are assembled in Table 1. Thus, the following overall processes take place in electrochemical facetting:

(i) For values of E_u more positive than the M^{z+}/M redox couple potential, the metal (M) selectively electrodissolves as M^{z+} and diffusion of M^{z+} species towards the solution takes place during the anodic

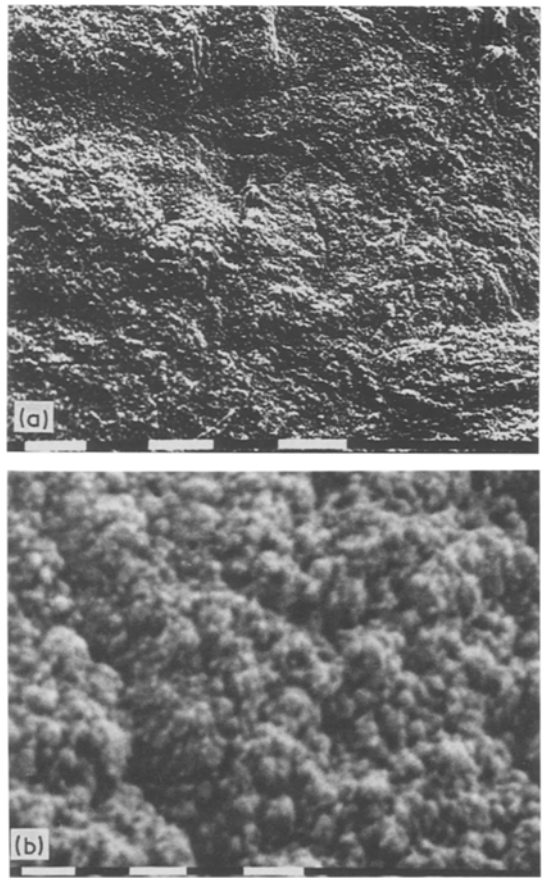

Fig. 9. SEM micrographs of a platinum electrode surface after electrochemical treatment according to Procedure (ii). R = 300, scale: (a) 10 μm; (b) 1 μm.

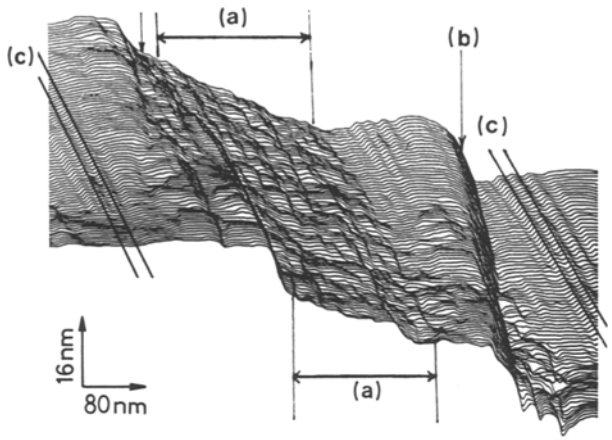

Fig. 10. STM image of a platinum electrode surface treated according to Procedure (ii). R = 40: (a) casket-like structure; (b) deep corrugated structure; (c) parallel ridge-like structure.

half-period, τ_u. Subsequently, at E_l, the complementary metal selective electrodeposition occurs during the cathodic half-period, τ_l.

(ii) The processes at E_u are the same as in (i) but the complementary selective electrodeposition reaction at $E_l \leqslant 0.4$ V occurs simultaneously with another electrochemical process such as, for instance, the H-adatom electroformation.

(iii) For the preset E_u values the formation of an oxide metal layer becomes possible. This layer can be either totally or partially electroreduced at E_l yielding a facetted surface usually accompanied by an increase in roughness.

In all cases, the frequency of the periodic perturbing potential plays a fundamental role as it determines the average thickness of the pulsating diffusion-boundary layer ($\langle\delta_p\rangle$) associated with the transport of the M^{z+} species in solution. The value of $\langle\delta_p\rangle$ decreases with the reciprocal of $f^{1/2}$ [37, 38]. It should be mentioned that the values of $\langle\delta_p\rangle$ for the electrodissolution and for the electrodeposition processes are, in fact, different, as can be seen through the corresponding concentration profiles obtained by solving Fick's diffusion equations with the proper boundary conditions [39]. This difference in $\langle\delta_p\rangle$ explains how soluble M^{z+} species accumulate in the solution near to the electrode surface during the electrochemical facetting [36], and through the transient concentration profiles information about the kinetics of the overall process can be derived [40].

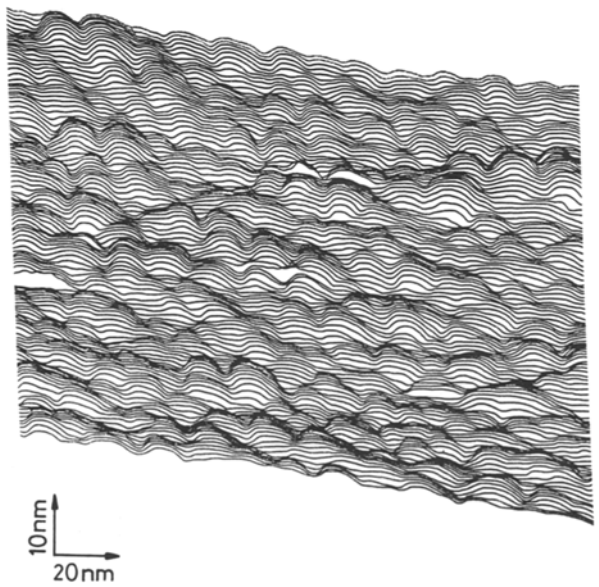

Fig. 11. STM image corresponding to the casket-like structure for treated platinum according to Procedure (ii). R = 60.

For low frequency perturbing potentials, that is, in the 0.025–0.1 kHz range, as $\langle\delta_p\rangle$ lies in the order of 10^{-3} cm [12, 37, 38], the overall electrochemical process turns out to be diffusion controlled. In this case for platinum, dendritic metal overlayers exhibiting a large active surface area are obtained. For higher frequencies, that is, in the 1–6 kHz range, $\langle\delta_p\rangle$ decreases to values between 10^{-4} and 10^{-5} cm [12, 37, 38] which are much smaller than those found for mass transport controlled reactions. Thus, the kinetics of the overall process changes progressively from diffusion to activation control and the electrodissolution and the electrodeposition processes occur selectively as they become strongly dependent on the physicochemical characteristics of each crystallographic face [11, 12, 30], namely work function, potential of zero charge, anion adsorbability and surface hydrophobicity. Under these conditions, the morphology of the treated surface changes gradually to that of a facetted surface with development of pco. Furthermore, the mean square displacement of adatoms on the surface ($\langle\Delta x^2\rangle$) depends on both the diffusion coefficient (D) of the adatom on each crystallographic face and the cathodic half-period of the periodic perturbing potential, that is, $\langle\Delta x^2\rangle = 2D\tau_l$ [41].

The precedent metal surface restructuring mechanism at relatively high frequency (0.5 kHz $\leqslant f \leqslant$ 50 kHz) has been successfully simulated through the Monte Carlo method [42]. The different stages of the overall process can be summarized as follows: (a) initial smoothing through the disappearance of macroroughness at prominent sites; (b) selective nucleation at definite growing sites resulting in the development of a particular type of crystallographic face; (c) development of a stabilized step-like morphology which involves a relatively thick restructured layer practically free of voids. This characteristic of the resulting metal overlayer explains the stability of the treated surfaces. Finally, (d) the influence of foreign adsorbates, such as H-adatoms, in defining the final surface atom arrangement. The presence of H-adatoms implies an interaction impeding the formation of the most densely packed (111) face and favours the development of (100), and eventually (110) faces. These conclusions are supported by STM images of the preferred oriented surfaces obtained at different times during the electrochemical treatment [30].

The electrochemical facetting mechanism predicts that when τ_l is sufficiently small so that $\langle\Delta x^2\rangle$ is not compatible with the distance between growing steps, the preferred orientation effect should be no longer observed. This is actually the case for platinum at

frequencies higher than 50 kHz [12]. Under these conditions the conventional faradaic processes can no longer follow the periodic potential perturbation and the modifications at the surface appear to be similar to those accomplished through thermal annealing.

5. The mechanism related to the formation of electrodispersed metal super-cluster-like electrode layer

The macroscopic growth of anodic oxide layers on many fcc metals (platinum, rhodium, gold) which are adequate for providing a marked increase in the active electrode area after their electroreduction, requires the application of a periodic perturbing potential between preset upper and lower potential limits at a frequency exceeding a certain threshold value. Likewise, the average potential of the fast periodic perturbing potential (see Section 2) results more positive than the equilibrium potentials of those redox reactions involving different metal oxide species [35]. (As an example for platinum, see Table 1). Under the above mentioned RSWPS conditions it should be expected that a net balance favouring the electrooxidation of the metal and the accumulation of a metal oxide layer occurs.

Otherwise, the anodic half-period, as deduced from the threshold value of the frequency ($f_{th} \approx 0.5$ kHz), must be smaller than 1 ms to promote the metal oxide layer growth. This time is shorter than the average half-life time of the $M(OH)_{ad}$ intermediate produced in the reversible underpotential decomposition of water on the metal electrode occurring in acids [43–46], according to the reaction

$$M + H_2O = M(OH)_{ad} + H^+ + e^- . \quad (1)$$

This means that any reaction of the $M(OH)_{ad}$ species implying a further irreversible deprotonation and simultaneous formation of more stable surface oxide species, such as ageing processes [45–47], can be neglected. Furthermore, on many fcc metals it was found that growth of the anodic oxide layers under fast periodic potentials only involves hydrous forms of metal hydroxide/oxide [1, 2, 10, 48, 49]. Thus, the formation of thick oxide layers under RSWPS can be interpreted in terms of a series of reversible reactions starting from the $M(OH)_{ad}$ intermediate, and finally yielding a non-aged hydrous metal oxide species. The different processes following Reaction (1) can be formally written according to the overall reaction

$$M(OH)_{ad} + (x + n - 1)H_2O = MO_n \cdot xH_2O + (2n - 1)H^+ + (2n - 1)e^- . \quad (2)$$

Likewise, the electroreduction half-cycle should mainly involve Reaction (1) in the reverse direction favouring the advance in depth of the metal plane and a partial contribution of the overall Reaction (2) through a reversible displacement of H^+ ions and H_2O molecules. Therefore, the RSWPS treatment under the suitable conditions already mentioned provides a thick hydrous oxide layer which, after proper electroreduction, yields the electrodispersed metal layer.

The overall hydrous oxide layer electroreduction process at low potential sweep rate apparently implies a 3D-nucleation and growth mechanism in the entire metal oxide [50], the final result being a large number of nearly spherical sticking metal super-clusters of about 10 nm average diameter such as were revealed by STM imaging [33, 34]. This type of cluster has already been observed for platinum, gold and palladium. The topography of the metal in these cases approaches that of periodic casket-like domains (Fig. 11) and this fact explains that the electroreflectance spectra of these electrodispersed metal layers for platinum and gold exhibit a band at an energy level lower than that of the corresponding mirror-polished surface [51].

The intriguing question concerning the same typical geometry and size of clusters for the different metals can be explained through the charge and potential distribution of metal clusters with an increasing number of atoms as resulting from quantum-mechanical calculations [52]. The latter show that the differences between atoms at distinguishable surface sites tend to disappear as the number of atoms increases. Consequently, a stable spherical shape for clusters can be approached, and the average diameter of clusters found in the electrodispersed metal electrodes can be associated with the minimum assemblage of metallic atoms compatible with bulk metal properties. This type of cluster involves a surface atom/volume atom ratio where enhanced catalytic properties for certain reactions are observed [53, 54]. Some applications in this respect are discussed later.

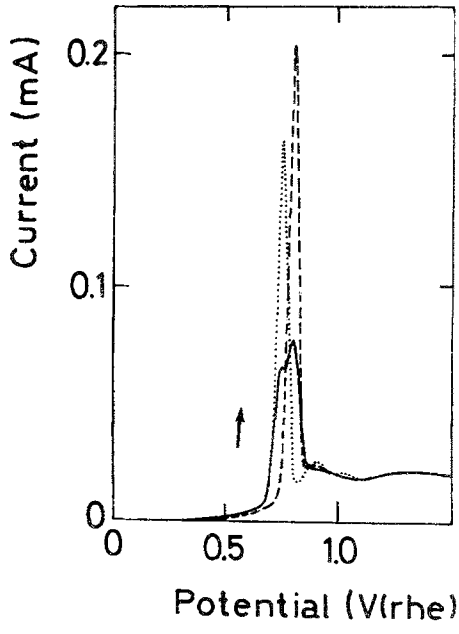

Fig. 12. Voltammograms at 0.1 V s^{-1} for adsorbed carbon monoxide electrooxidation on platinum in 0.05 M $HClO_4$; 25° C. Full trace corresponds to pc platinum. Dotted line belongs to (111)-type preferentially oriented platinum. Dashed line denotes (100)-type preferentially oriented platinum. Adsorption potential: 0.25 V; adsorption time: 1 min.

6. Some electrocatalytic reactions on modified metal electrodes

The electrochemical behaviour of modified metal electrodes can be illustrated through various examples recently reported in the literature.

6.1. *Electrooxidation of adsorbed CO on preferentially oriented platinum electrodes*

The electrooxidation of CO preadsorbed on both (100)-type and (111)-type preferentially oriented platinum yielding CO_2 was investigated by applying a flowcell electrochemical technique [55]. At a low potential sweep rate the electrooxidation reaction in 0.05 M $HClO_4$ exhibited a sharp peak at about 0.8 V (against reversible hydrogen electrode potential) for the reaction taking place at the (100)-type preferentially oriented platinum and another peak at about 0.7 V for the (111)-type preferentially oriented platinum (Fig. 12). These results explain, in principle, the intriguing peak multiplicity previously reported for this reaction at polycrystalline platinum electrodes in acid electrolytes.

6.2. *Adsorption and electrooxidation of ethylene on large surface area electrodispersed platinum electrodes*

The adsorption and electrooxidation of ethylene in 1 M H_2SO_4 were recently studied on both conventional platinized platinum and electrodispersed platinum electrodes [32]. The final products of the electrooxidation reaction were CO_2 and H^+ ions. The maximum ethylene surface coverage in the 40–80° C range was practically independent of both roughness factor (r) and electrode structure. However, the time to attain the stationary ethylene surface coverage at the potential of maximum ethylene adsorption was significantly larger on porous highly platinized platinum electrodes than that on electrodispersed platinum electrodes of similar or larger roughness factor (Fig. 13). This difference in the adsorption times was attributed to kinetic hindrances caused by the porous structure of platinized platinum electrodes.

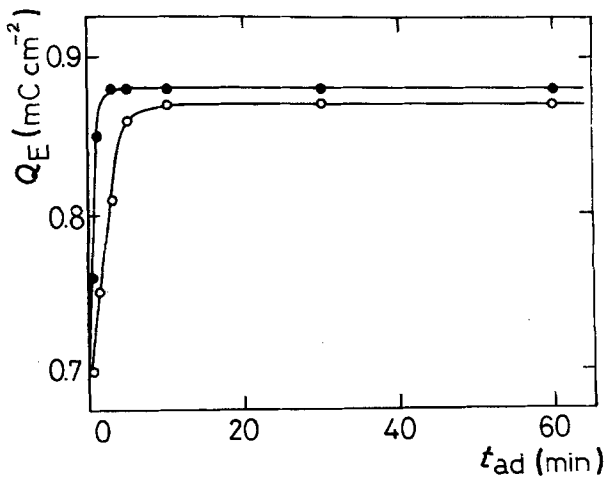

Fig. 13. Dependence of the charge related to the adsorbed ethylene electrooxidation (Q_E) on the adsorption time (t_{ad}) at 0.25 V (against r.h.e.); 1 M H_2SO_4; 40° C: (●) electrodispersed platinum electrode; R = 320. (○) conventional platinized platinum electrode; R = 170.

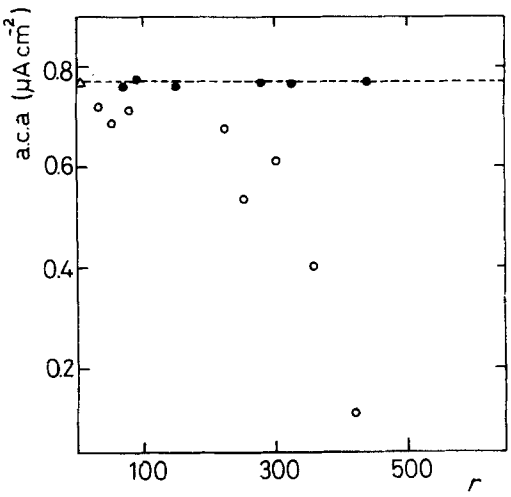

Fig. 14. Dependence of the apparent specific catalytic activity (aca) on the roughness factor for differently prepared platinum electrodes; 1 M H_2SO_4, 80° C: (△) smooth platinum electrode; (●) electrodispersed platinum electrodes; (○) conventional platinized platinum electrode.

On the other hand, a clear dependence of the apparent specific catalytic activity (aca) for the steady-state electrooxidation of ethylene on platinum electrode structure was observed (Fig. 14). Thus, platinized platinum electrodes exhibit a low aca which decreases on increasing the roughness factor due to additional overpotential contributions within the pores. Conversely, for electrodispersed platinum the aca is practically independent of the roughness factor and the average value of the aca is equal to that resulting for the uniformly polarized smooth platinum.

6.3. *Electrooxidation of reduced CO_2 on large surface area electrodispersed platinum electrodes*

The electrooxidation of 'reduced' CO_2 preadsorbed on electrodispersed platinum in 0.5 M H_2SO_4 was recently investigated through voltammetry [56]. This reaction is associated with a voltammetric peak at 0.65 V which comprises a charge of about one adsorbate monolayer (Fig. 15).

The voltammetric peak appears at a potential lower than that observed for smooth platinum. This clear depolarization effect for the reaction correlates with the greater electrocatalytic activity of these electrodes for the stationary electrooxidation of methanol and formic acid in the same electrolytes as compared to conventional platinum electrodes [57]. The explanation of the depolarizing effect must be sought through the proper structure of these electrodes, particularly the crystallite size of the particles. In heterogeneous catalysis the influence of the crystallite size on the chemisorption of reactants sensitive to the catalyst structure is well-known. In this respect the platinum particles of about 10 nm diameter can be regarded as incomplete

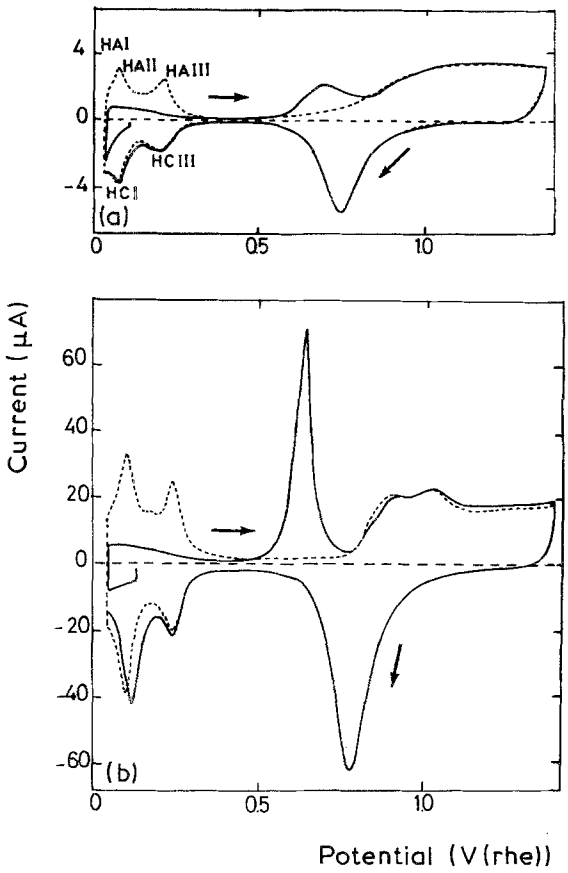

Fig. 15. Voltammograms at 5×10^{-3} V s^{-1} corresponding to the electrooxidation of 'reduced' carbon dioxide on platinum in 0.5 M H_2SO_4 at 25° C (full traces): (a) conventional polished pc platinum; (b) electrodispersed platinum, R = 37. Dashed lines correspond to the blanks.

cubooctahedrons in which the relative number of edge and corner atoms with respect to the total number of atoms lies close to the optimal situation compatible with the metallic character of the electrode material [53, 54].

In conclusion, large surface area electrodispersed platinum electrodes behave, for relatively small size reactants such as H-atoms, O-atoms, CO, C_2H_4, etc., without porosity interference in the kinetics of electrocatalytic reactions of adsorbates and exhibit, in many of these cases, a depolarization effect which can be correlated to the electrode structure previously established through SEM and STM imaging.

Acknowledgements

This work was financially supported by the Consejo Nacional de Investigaciones Científicas y Técnicas of Argentina and the Comisión de Investigaciones Científicas de la Provincia de Buenos Aires. W. E. Triaca thanks the Third World Academy of Sciences for Research Grant No. 87-15. STM images shown in this work were taken at the facilities available at the Departamento de Física Fundamental, Universidad Autónoma, Madrid, Spain. The cooperative work with Professor N. García and A. Baró is acknowledged.

References

[1] A. C. Chialvo, W. E. Triaca and A. J. Arvia, *J. Electroanal. Chem.* **146** (1983) 93.
[2] *Idem, ibid.* **171** (1984) 303.
[3] J. C. Canullo, W. E. Triaca and A. J. Arvia, *ibid.* **175** (1984) 337.
[4] R. M. Cerviño, W. E. Triaca and A. J. Arvia, *ibid.* **182** (1985) 51.
[5] *Idem, J. Electrochem. Soc.* **132** (1985) 266.
[6] E. Custidiano, A. C. Chialvo and A. J. Arvia, *J. Electroanal. Chem.* **196** (1985) 423.
[7] C. L. Perdriel, M. Ipohorski and A. J. Arvia, *ibid.* **215** (1986) 317.
[8] E. Custidiano, T. Kessler, W. E. Triaca and A. J. Arvia, *Electrochim. Acta* **31** (1986) 1671.
[9] W. E. Triaca, T. Kessler, J. C. Canullo and A. J. Arvia, *J. Electrochem. Soc.* **134** (1987) 1165.
[10] A. C. Chialvo, W. E. Triaca and A. J. Arvia, *J. Electroanal. Chem.* **237** (1987) 237.
[11] A. J. Arvia, J. C. Canullo, E. Custidiano, C. L. Perdriel and W. E. Triaca, *Electrochim. Acta* **31** (1986) 1359.
[12] A. Visintin, J. C. Canullo, W. E. Triaca and A. J. Arvia, *J. Electroanal. Chem.* **239** (1988) 67.
[13] A. Visintin, W. E. Triaca and A. J. Arvia, *ibid.* **221** (1987) 239.
[14] J. C. Canullo, W. E. Triaca and A. J. Arvia, *ibid.* **200** (1986) 397.
[15] E. Custidiano, A. C. Chialvo, M. Ipohorski, S. M. Piovano and A. J. Arvia, *ibid.* **221** (1987) 229.
[16] J. C. Canullo, E. Custidiano, R. C. Salvarezza and A. J. Arvia, *Electrochim. Acta* **32** (1987) 1649.
[17] A. C. Chialvo, W. E. Triaca and A. J. Arvia, *Anal. Assoc. Quím. Arg.* **73** (1985) 23.
[18] J. Clavilier, R. Durand, G. Guinet and R. Faure, *J. Electroanal. Chem.* **127** (1981) 281.
[19] C. L. Scortichini and C. N. Reilley, *ibid.* **139** (1982) 233.
[20] J. Clavilier, D. Armand, S. G. Sun and M. Petit, *ibid.* **205** (1986) 267.
[21] A. V. Tripković and R. R. Adžić, *ibid.* **205** (1986) 335.
[22] F. G. Will, *J. Electrochem. Soc.* **112** (1965) 451.
[23] P. N. Ross, Jr., *J. Electroanal. Chem.* **76** (1977) 139.
[24] A. T. Hubbard, R. M. Ishikawa and J. Katekaru, *ibid.* **86** (1978) 271.
[25] K. Yamamoto, D. M. Kolb, R. Kötz and G. Lehmpfuhl, *ibid.* **96** (1979) 233.
[26] P. N. Ross, Jr., *J. Electrochem. Soc.* **126** (1979) 67.
[27] J. Clavilier, R. Faure, G. Guinet and R. Durand, *J. Electroanal. Chem.* **107** (1980) 205.
[28] F. E. Woodward, C. L. Scortichini and C. N. Reilley, *J. Electroanal. Chem.* **151** (1983) 109.
[29] R. M. Cerviño, A. J. Arvia and W. Vielstich, *Surf. Sci.* **154** (1985) 623.
[30] J. Gómez, L. Vásquez, A. M. Baró, N. García, C. L. Perdriel, W. E. Triaca and A. J. Arvia, *Nature* **323** (1986) 612.
[31] L. Vásquez, J. M. Gómez Rodriguez, J. Gómez Herrero, A. M. Baró, N. García, J. C. Canullo and A. J. Arvia, *Surf. Sci.* **181** (1987) 98.
[32] S. M. Piovano, A. C. Chialvo, W. E. Triaca and A. J. Arvia, *J. Appl. Electrochem.* **17** (1987) 147.
[33] L. Vásquez, J. Gómez, A. M. Baró, N. García, M. L. Marcos, J. González-Velasco, J. M. Vara Cuadrado, A. J. Arvia, J. Presa, A. García and M. Aguilar, *J. Am. Chem. Soc.* **109** (1987) 1730.
[34] J. Gómez, L. Vásquez, A. M. Baró, C. Alonso, E. González, J. González-Velasco and A. J. Arvia, *J. Electroanal. Chem.*, **240** (1988) 77.
[35] 'Standard Potentials in Aqueous Solutions', edited by A. J. Bard, R. Parson and J. Jordan, Marcel Dekker, New York (1985).
[36] C. L. Perdriel, W. E. Triaca and A. J. Arvia, *J. Electroanal. Chem.* **205** (1986) 279.
[37] A. R. Despić and K. I. Popov, *J. Appl. Electrochem.* **1** (1971) 275.
[38] N. Ibl, *Surf. Technol.* **10** (1980) 81.
[39] S. L. Marchiano, L. Rebollo Neira and A. J. Arvia, *Electrochim. Acta.*, in press.

[40] C. L. Perdriel, E. Custidiano and A. J. Arvia, *J. Electroanal. Chem.*, in press.
[41] A. J. Bard and L. F. Faulkner, 'Electrochemical Methods', John Wiley, New York (1980).
[42] E. V. Albano, H. O. Mártin and A. J. Arvia, *Physical Review B* **35** (1987) 9341.
[43] B. E. Conway, H. Angerstein-Kozlowska, F. C. Ho, J. Klinger, B. MacDougall and S. Gottesfeld, *Faraday Discuss. Chem. Soc.* **56** (1973) 210.
[44] C. M. Ferro, A. J. Calandra and A. J. Arvia, *J. Electroanal. Chem.* **59** (1975) 239.
[45] C. D. Pallotta, N. R. de Tacconi and A. J. Arvia, *Electrochim. Acta* **26** (1981) 261.
[46] *Idem*, *J. Electroanal. Chem.* **159** (1983) 201.
[47] M. E. Folquer, J. O. Zerbino, N. R. de Tacconi and A. J. Arvia, *J. Electrochem. Soc.* **126** (1979) 592.
[48] L. D. Burke and T. A. M. Twomey, *J. Electroanal. Chem.* **162** (1984) 401.
[49] A. Visintín, A. C. Chialvo, W. E. Triaca and A. J. Arvia, *ibid.* **225** (1987) 227.
[50] A. M. Castro Luna, A. Visintín, A. E. Bolzán, R. C. Salvarezza and A. J. Arvia, *Electrochim. Acta.*, **33** (1988) 1743.
[51] R. O. Lezna, N. R. de Tacconi, C. L. Perdriel and A. J. Arvia, 171st Meeting, The Electrochemical Society, Philadelphia, USA, May 10–15, Abst. 508, p. 726 (1987).
[52] E. E. Mola, J. L. Vicente, E. Custidiano and A. J. Arvia, Langmuir, **4** (1988) 1142.
[53] O. M. Poltorak and V. S. Boronin, *Russ. J. Phys. Chem.* **40** (1966) 1436.
[54] P. Stonehart, K. Konoshita and J. A. S. Bett, 'Proc. Electrocatalysis' (Edited by M. W. Breiter), The Electrochemical Society, Princeton (1984), p. 275.
[55] E. P. M. Leiva, E. Santos, M. C. Giordano, R. M. Cerviño and A. J. Arvia, *J. Electrochem. Soc.* **133** (1986) 1660.
[56] M. L. Marcos, J. M. Vara, J. González-Velasco, M. C. Giordano and A. J. Arvia, *J. Electroanal. Chem.* **270** (1989) 205.
[57] A. M. Castro Luna, M. C. Giordano and A. J. Arvia, *J. Electroanal. Chem.* **259** (1989) 173.